Broadband terahertz spectroscopy

(Invited Paper)

Wenhui Fan (范文慧)

State Key Laboratory of Transient Optics and Photonics, Xi'an Institute of Optics and Precision Mechanics, Chinese Academy of Sciences, Xi'an 710119, China

Corresponding author: fanwh@opt.ac.cn

Received September 9, 2011; accepted September 22, 2011; posted online October 24, 2011

An overview of the major techniques to generate and detect THz radiation so far, especially the major approaches to generate and detect coherent ultra-short THz pulses using ultra-short pulsed laser, has been presented. And also, this paper, in particularly, focuses on broadband THz spectroscopy and addresses on a number of issues relevant to generation and detection of broadband pulsed THz radiation as well as broadband time-domain THz spectroscopy (THz-TDS) with the help of ultra-short pulsed laser. The time-domain waveforms of coherent ultra-short THz pulses from photoconductive antenna excited by femtosecond laser with different pulse durations and their corresponding Fourier-transformed spectra have been obtained via the numerical simulation of ultrafast dynamics between femtosecond laser pulse and photoconductive material. The origins of fringes modulated on the top of broadband amplitude spectrum, which is measured by electric-optic detector based on thin nonlinear crystal and extracted by fast Fourier transformation, have been analyzed and the major solutions to get rid of these fringes are discussed.

OCIS codes: 300.6495, 300.6270, 040.2235, 320.7160.
doi: 10.3788/COL201109.110008.

1. Introduction

Spanning the frequency range between the infrared (IR) radiation and microwaves, terahertz (THz) waves are, also known as T-rays, T-lux, or simply called THz, assigned to cover the electromagnetic spectrum typically from 100 GHz (10^{11} Hz) to 10 THz (10^{13} Hz), namely, from 3 mm to 30 μm in wavelength, although slightly different definitions have been quoted by different authors. For a very long time, THz region is an almost unexplored field due to its rather unique location in the electromagnetic spectrum. Well-known techniques in optical or microwave region can not be directly employed in the THz range because optical wavelengths are too short and microwave wavelengths are too long compared to THz wavelengths.

With the rapid technological innovation in photonics and other modern technologies, such as ultra-short pulsed laser, micromachining and nanotechnology, new techniques in the THz region came out continuously and speeded up this "almost unexplored" field emerging in our life. Nowadays, THz research are walking into the "New Spring" with many very promising and important applications discovered until recently, such as information and communications technology, biology and medical sciences, pharmaceuticals, non-destructive evaluation, material characterization, homeland security, on-line quality control, environmental monitoring, and so on.

Today, a number of characteristics have been found in the THz region. Firstly, THz radiation is non-ionizing[1] with very low photon energy, 4 meV corresponding to 1 THz, which is far below the threshold energies to break chemical bonds or to cause gene mutations, and thus, it should be harmless for the application of THz waves to human tissue. Secondly, THz waves have the capability to pass through a wide variety of non-conducting materials, such as clothing, paper, dry wood, plastic, and also go easily through smoke or dust with the small particle size, although they have the strong reflection by metal and huge absorption by water. Generally speaking, nonpolar, dry, and nonmetallic materials are transparent or translucent to THz waves. Therefore, weapons concealed beneath clothing or products contained in plastic packages can be seen by THz waves. This transparency motivates the utilization of THz waves in quality control and security applications[2−5]. Even the strong absorption of THz energy by water has merits in biology science because THz waves are highly sensitive to the hydration level in biological tissue[6,7].

Thirdly, most polar molecules either in the solid or liquid phase show the characteristic "fingerprint" absorption by absorbing unique THz energies corresponding to their vibrational transitions[8−11], and polar molecules in the gas phase also have their rotational transition energies spanning the microwave and THz frequencies[12−14]. Therefore, the absorption spectrum across THz range by means of THz spectroscopy permits specific detection, such as material characterization, classification or recognition[15,16]. On the other hand, plasma frequencies and damping rates of moderately doped semiconductors also locate in the THz region between 0.1 and 2.0 THz[17,18], and they are proportional to the carrier density and mobility of semiconductors, respectively. Thus, time-resolved THz spectroscopy is an ideal tool for the study of carrier dynamics in semiconductors. Moreover, THz waves can be also employed to stimulate Rabi oscillations in two-level impurity states in semiconductors, which enable the manipulation of physical qubits[19−21]. Furthermore, the Josephson plasma frequency of high-T_c cuprate superconductors, such as $Bi_2Sr_2CaCu_2O_8$, lie at

sub-THz frequency region, which allows us to investigate charge dynamics in this extremely anisotropic superconductor, and opens up the possibility to study other highly correlated systems in this critical low-energy region[22]. Also, the Cyclotron frequency of most semiconductor superlattices applied simultaneously by strong electric field and magnetic field were found to lie at terahertz region[23].

THz technology is now growing very rapidly in many fields, numerous recent breakthroughs, such as THz radiation generated by laser-induced gas plasma[24−26], THz quantum-cascade laser (THz–QCL)[27−29], THz metamaterials[30−32], have pushed THz research into the central stage. Here, this paper will particularly focus on broadband THz spectroscopy and address on a number of issues relevant to generation and detection of broadband pulsed THz radiation as well as broadband time-domain THz spectroscopy (THz–TDS).

2. Generation and detection of THz radiation

Sitting at the boundaries of microwave and photonic technology, THz technology is quite underdeveloped compared with the achievements in microwave or photonics due to the difficulties in generation and detection of THz radiation efficiently as well as high atmospheric absorption. However, the location of the THz frequency range between the electronic and photonic domains implies that optical or electronic, or even a mixture of optical and electronic methods, can be employed for generation and detection of THz waves. So far, a number of techniques have been utilized to generate and detect THz radiation, such as electronic devices, free-electron laser, gas laser, p-type germanium laser, difference-frequency generation or optical parametric oscillation, photo-mixing, quantum cascade laser, laser-induced plasma, ultra-short pulsed laser, and so on. Among these techniques, optical generation and detection of sub-picosecond single cycle THz transients with the help of femtosecond laser pulses is one of the most significant milestones in the exploration of THz region and has gained widespread acceptance as a convenient method access to THz frequencies.

Nowadays, the THz region has become more accessible due to the significant advancement in solid-state ultrashort pulsed lasers and coherent "time-gated" detection scheme based on ultra-short pulsed lasers, which could generate and detect free space coherent pulsed THz radiation with very high signal-to-noise ratio (SNR) at room temperature and insensitive to the thermal background.

For the generation of coherent ultra-short THz pulses, two major approaches relying on ultra-short laser pulses have been developed continuously. The first approach mainly focuses on photoconductive (PC) antenna fabricated by semiconductors, which is proved as a good THz source with excellent intensity and bandwidth properties[33], and involves generating an ultrafast photocurrent on PC antenna using electric-field carrier acceleration. The second approach generates THz waves via nonlinear optical effects, such as optical rectification (OR), using femtosecond laser excitation. From the point of view of efficiency, simplicity, and diversity of possible applications, optical rectification of ultrashort laser pulses is currently the most promising method for generation of high-energy THz pulses. The high-power broadband coherent THz generation through optical rectification using the tilted-pulse-front excitation has been achieved recently[34], which could be able to produce THz pulses having 1 000 times larger energy than that of THz pulses generated in ZnTe crystal by using the same pump pulse energy. Furthermore, an intriguing approach, ambient air-plasma generation based on amplified femtosecond laser[25,26], appears not long ago and is drawing considerable attention at present, particularly with respect to security applications.

As for the detection of coherent pulsed THz radiation using femtosecond laser, time-gated PC antenna made by low-temperature-grown GaAs (LTG-GaAs) and time-gated electro-optic (EO) detector based on electro-optic sampling (EOS) technique using a piece of nonlinear zinc blende crystal, such as ZnTe, GaSe, GaP, have been extensively studied and utilized. Unlike time-gated PC antenna, the EO crystals used in time-gated EO detector are readily commercially available and do not require micro-fabrication techniques to make them, so it became the relatively popular choice for THz detection. Other conventional THz detectors, such as helium-cooled bolometers, goley cells, deuterated triglycine sulphate (DTGS) crystals, Schottky barrier diodes (SBDs), superconduductor-insulator-superconductor (SIS) junctions, even pyroelectric detector, are also available for the detection of THz radiation. It should be noted that the key advantage of the time-gated THz detection based on femtosecond laser over the conventional THz detectors is the inherent suppression of the thermal background, and it is the coherent detection, namely, the amplitude and phase of THz signal could be measured simultaneously.

Moreover, it is worthy to be mentioned, several interesting techniques and devices, such as THz radiation enhanced emission of fluorescence (THz-REEF)[35] and THz quantum well infrared photodetectors (THz-QWIPs)[36], come out recently and are improved steadily. Furthermore, a THz-single-photon detector has also been developed using a single-electron transistor[37].

3. Broadband THz time-domain spectroscopy

As mentioned above, THz radiation possesses a unique combination of desirable properties for non-destructive imaging and spectroscopy of materials. For example, the characteristic spectral features exhibited by many materials across the THz frequency range is of particular interest for the applications of quality assurance and security technologies related with material characterization, classification or recognition[38]. Therefore, THz spectroscopy can be used as a suitable tool to uniquely identify specific chemicals possessing intramolecular vibrational modes and intermolecular vibrations. The significant breakthrough in this field is the progress of femtosecond lasers in conjunction with the utilization of time domain spectroscopy (TDS) in a coherent detection scheme, which is currently called THz time-domain spectroscopy (THz-TDS).

As a particular sensitive tool for many applications that are very hard to carry out by traditional inco-

herent Fourier transform far-IR spectroscopy (FTIR), THz-TDS has many unique features, such as coherent detection (amplitude and phase could be measured simultaneously, enabling both the absorption coefficient and the refractive index to be calculated directly without using the Kramers-Kronig relation), sub-picosecond temporal resolution (time-resolved THz spectroscopy is suitable for the study of carrier dynamics in semiconductors with ultrahigh time resolution) and time-gated detection (THz pulses carrying the spectral information are sampled by means of the femtosecond laser pulses so that the inherent suppression of the thermal background can be achieved), and plays a very crucial role for many important applications, such as non-destructive testing and monitoring, online process control, extremely high time resolution dynamics, sensing and imaging, and so on.

The schematic representation of the typical THz-TDS experimental apparatus is shown in Fig. 1. A diode-pumped ultra-short pulsed Ti: sapphire laser provides near-infrared (NIR) femtosecond pulses at a center wavelength around 800 nm with a repetition rate of 76 MHz and is used as the light source of THz-TDS setup. The output laser beam is normally split into a pump beam (∼90%) and a probe beam (∼10%) by a beam splitter (BS). Coherent ultra-short THz pulses are generated by focusing the pump beam onto the gap of a biased PC antenna fabricated by LTG-GaAs. The pulse duration of the pump laser incident on the PC antenna can be measured by autocorrelator and is approximately from tens of femtoseconds to 100 femtoseconds after passing through a number of optical components. The pulsed THz radiation generated from the PC antenna is collected and then focused by a pair of Au-coated off-axis parabolic mirrors onto the sample. A second pair of Au-coated off-axis parabolic mirrors collects the transmitted THz radiation and focuses it onto a piece of EO crystal, which is mounted collinearly with the NIR probe beam for coherent detection. The time-domain electric field comprising the THz waveform is measured using EOS and a lock-in detection scheme. The corresponding frequency-domain amplitude THz spectrum can be extracted by fast Fourier transformation (FFT). The typical Fourier-transformed THz spectrum of dry nitrogen is shown in Fig. 2.

At present, the typical THz-TDS apparatus mainly utilizes either the PC antenna fabricated by semiconductors or the nonlinear crystals based on optical rectification

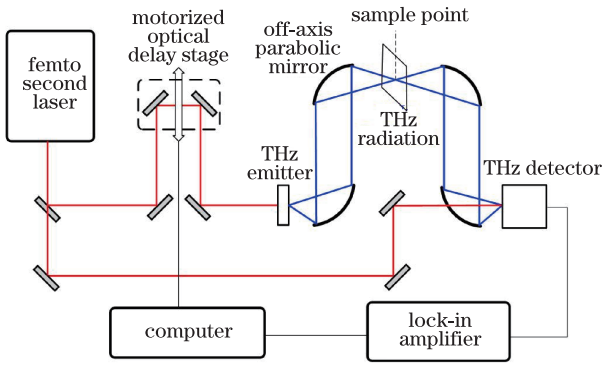

Fig. 1. Schematic of the typical THz-TDS experimental apparatus.

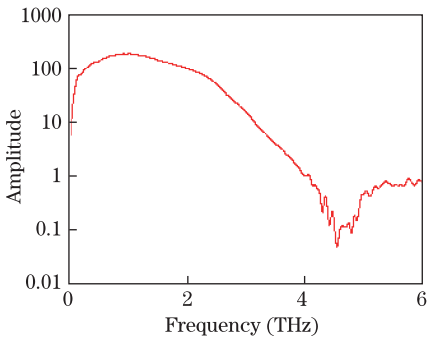

Fig. 2. Typical Fourier-transformed THz spectrum of dry nitrogen.

for THz generation and photoconductive sampling (PCS) or the nonlinear crystals based on free space electro-optic sampling (FS-EOS) for THz detection. But, the majority of THz-TDS studies reported is confined to the limited frequency range, 0.1–3 THz. In order to further improve the accuracy of identification for specific chemicals or materials, it is quite necessary to develop the THz-TDS technique with broader bandwidth and good SNR. Obviously, more clearly characteristic spectral features are measured, better identification of specific chemicals are achieved.

4. Broadband THz generation

To generate the broadband pulsed THz radiation, ultra-short pulsed laser is essential and other critical factors should also be considered. Here, the broadband pulsed THz radiation generated by PC antenna is analyzed for clarification. In fact, in order to achieve the better output power and broader bandwidth for THz radiation generated from PC antenna, some key factors, such as pulse power and pulse duration of pump laser, biased electric field on PC antenna, the photoconductive materials used as the substrate of PC antenna, have to be carefully chosen and optimized by considering the following equations deduced from the fundamental theory on electromagnetic radiation and Maxwell's equations:

$$E_{\mathrm{THz}}(t) = -\frac{L}{4\pi\varepsilon_0 c^2 z}\frac{\mathrm{d}}{\mathrm{d}t}J(t) \propto \frac{\mathrm{d}}{\mathrm{d}t}J(t). \tag{1}$$

The first time derivative of time-varying transient photocurrent $J(t)$ can be written as

$$\frac{\mathrm{d}}{\mathrm{d}t}J(t) = \frac{\mathrm{d}}{\mathrm{d}t}[en(t)v(t)] = ev(t)\frac{\mathrm{d}n(t)}{\mathrm{d}t} + en(t)\frac{\mathrm{d}v(t)}{\mathrm{d}t}. \tag{2}$$

Here, the first time derivative of time-varying transient photocarriers $n(t)$ can be written as

$$\frac{\mathrm{d}n(t)}{\mathrm{d}t} = -\frac{n(t)}{\tau_{\mathrm{c}}} + n_0 \exp\Big(-\frac{t^2}{\delta_t^2}\Big), \tag{3}$$

where τ_{c} is the lifetime of photocarriers, δ_t is the pulse duration of pump laser, and the maximum number of photocarriers n_0 can be written as

$$n_0 = \frac{1}{h\nu}P_0, \tag{4}$$

where P_0 is the peak power of pump laser excited on the PC antenna.

Furthermore, the time-varying relative velocity $v(t)$ is the difference of the velocity of hole $v_{\rm h}(t)$ and the velocity of electron $v_{\rm e}(t)$, namely, $v(t) = v_{\rm h}(t) - v_{\rm e}(t)$.

The first time derivative of the relative velocity $v(t)$ can be written as

$$\frac{{\rm d}v(t)}{{\rm d}t} = -\frac{v(t)}{\tau_{\rm s}} + \frac{m_{\rm e}^* + m_{\rm h}^*}{m_{\rm e}^* m_{\rm h}^*} e\Big[E_{\rm b} - \frac{P(t)}{3\varepsilon_0}\Big], \qquad (5)$$

where $E_{\rm b}$ is the external biased electric field, $\tau_{\rm s}$ is the relaxation time, $m_{\rm e}^*$ and $m_{\rm h}^*$ are the effective mass of hole and electron, respectively. $P(t)$ is the intensity of polarization.

It is clearly indicated by Eq. (2) that there are two ultrafast processes to make the contribution for enhancing THz electric field. One is relevant to the time-varying transient carrier density, i.e. the first part in Eq. (2), and another comes from the acceleration of photocarriers under the electric field, which is the second part in Eq. (2). The numerical simulation of these two ultrafast processes shows that the contribution relevant to the time-varying transient carrier density could be ten times bigger than that of the acceleration of photocarriers under the electric field. Therefore, THz electric field generated by PC antenna should be mainly dominated by the time-varying transient carrier density of PC antenna.

Moreover, the time-domain waveforms of coherent ultra-short THz pulses from PC antenna excited by femtosecond laser with different pulse durations and their Fourier-transformed spectra have also been calculated via the numerical simulation of ultrafast dynamics between femtosecond laser pulse and photoconductive material. More specifically, Fig. 3 depicts the waveforms of coherent ultra-short THz pulses versus different pulse durations of pump laser, and their corresponding Fourier-transformed spectra are shown in Fig. 4.

As shown in Fig. 3, the time-domain THz pulses are getting wider as the pulse durations of pump laser increasing, and the negative peaks of THz pulses become bigger, corresponding to the decline of photocurrent. Figure 4 shows the spectral bandwidths of THz radiation change inversely with the pulse durations of pump laser,

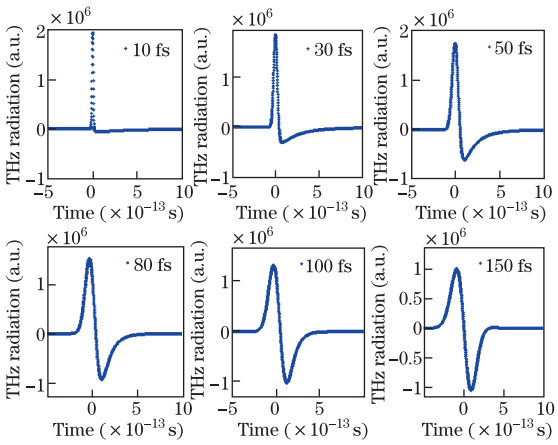

Fig. 3. Time-domain waveforms of coherent ultra-short THz pulses versus different pump pulse durations.

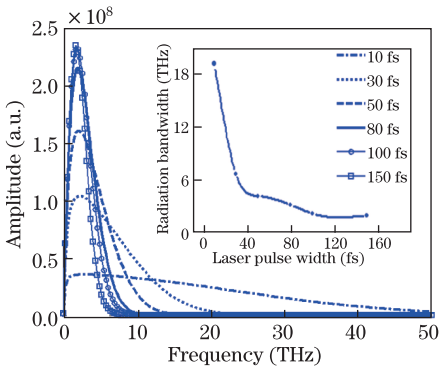

Fig. 4. Corresponding Fourier-transformed spectra of THz pulses versus different pump pulse durations.

which is clearly indicated that broadband THz radiation can be achieved from PC antenna by using ultra-short laser pulse. Furthermore, this phenomenon is also the clear evidence that the photocurrent pulse generated by pump laser will be changed dramatically when the pulse duration of pump laser is changed.

According to Eq. (3), it is clearly indicated that two key parameters, τ_c and δ_t, are very important to generate a very short photocurrent pulse. In fact, the photoconductor with very short lifetime carriers is more critical to obtain the very short photocurrent pulse, namely, if you cannot find a photoconductor with very short lifetime carriers, you cannot obtain a very short photocurrent pulse even you use a very short pulse duration laser. In other words, by irradiating the ultrafast photoconductor with ultra-short laser pulse, it will generate a very short photocurrent pulse.

5. Broadband THz characterization

In order to characterize the broadband pulsed THz radiation successfully, ultra-short pulsed laser is also essential and different issues should be considered more carefully for PCS or FS-EOS, respectively.

For the broadband pulsed THz radiation characterized by PCS, the performance of PC antenna for broadband pulsed THz detection is mainly dominated by the PC material. As far as SNR concerned, the PC antenna fabricated by PC material with shorter lifetime is superior to the PC antenna fabricated by PC material with longer lifetime, because the background noise of the PC material with longer lifetime is bigger than that of the PC material with shorter lifetime. Therefore, the SNR of PC antenna fabricated by LTG-GaAs (lifetime around 0.4 ps) is normally superior to the PC antenna fabricated by semi-insulating GaAs (SI-GaAs), of which lifetime is about 36 ps.

For the broadband pulsed THz radiation characterized by FS-EOS, both the detected THz signals and the detecting optical pulses (probe pulse) overlap and then pass through the nonlinear crystal, leading to the specially pre-polarized probe pulses with the THz field-induced phase retardation, which is proportional to the electric field strength of the detected THz signals, so phase matching between the detecting optical pulses and the detected THz signals is the big issue to be considered. Moreover, because the nonlinear crystals suitable for the

THz detection based on FS-EOS have strong optical phonon resonances in the THz range, the strong dispersion of THz refractive index limits the phase-matching frequency range. Thus, thick nonlinear EO crystals can only provide the detected THz signals and the detecting optical pulses with limited phase matching around a narrow frequency band, although the peak signal strength detected by thick EO crystal is normally higher than that by thin nonlinear EO crystals, which can provide better THz-optical phase matching within the full bandwidth of the detecting laser pulse. However, although thin EO crystal can provide good phase matching between the detected THz signals and the detecting optical pulses, leading to the considerable application for detecting broadband THz radiation, one of the practical problems should be pointed out if thin EO crystal is utilized directly to characterize broadband THz radiation.

In practice, the refractive index mismatch at the interface of thin EO crystal and air will lead to the phenomena that the detected THz signal trace contains multiple time delayed reflections of the main THz pulse, as shown in Fig. 5.

These multiple time delayed reflections of the main THz pulse, related to the THz pulse back-reflections inside the detecting EO crystal, will appear frequently in the time-domain scans with the time intervals ΔT approximately equal to

$$\Delta T = 2n_{\mathrm{g}}\frac{d}{c}, \tag{6}$$

where n_{g} is the group THz refractive index of the EO crystal, d is the thickness of the EO crystal, and c is the speed of light in vacuum.

When the spectroscopic information is extracted from the time-domain THz signal by FFT, these multiple time delayed reflections of the main THz pulse will produce modulation or fringes in the amplitude spectrum of the detected THz pulse with the frequency intervals $\Delta f_{\mathrm{fringe}}$, shown as

$$\Delta f_{\mathrm{fringe}} = \frac{1}{\Delta T}. \tag{7}$$

Figure 6 reveals these modulation or fringes appear in the frequency-domain amplitude spectrum of the detected THz pulse when the detected time-domain THz signal trace containing multiple time delayed reflections of the main THz pulse is directly extracted by FFT. Obviously, these needless modulation or fringes disturb seriously the real spectroscopic information obtained from

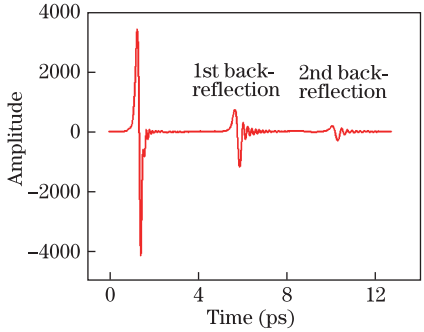

Fig. 5. Time-domain waveform of coherent ultra-short THz pulse with multiple time delayed reflections.

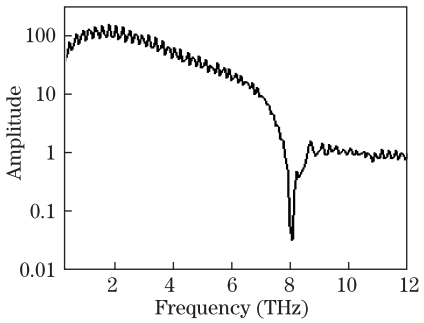

Fig. 6. Corresponding Fourier-transformed spectra with fringes appeared.

the extracted spectrum by FFT, since the weak spectral features can be hidden or undetectable. Furthermore, the Fourier-transformed THz spectrum modulated by these fringes will also lead to strong oscillations in the dynamic range of the THz-TDS setup, which affects the accuracy of absorption coefficient.

Generally, there are three major approaches for solving the problem of THz pulse reflections in the EO detector, especially for the thin EO crystal detecting the broadband THz signal. The first is the introduction of dielectric quarter-wave-thick ($\lambda/4$) layer in order to get rid of the multiple time delayed reflections completely. But, this is only suitable for the specific narrow band frequency range, which requires a dielectric layer with the relatively fixed thickness. For the frequency range from 0.1 to 10 THz, it would be very hard for a dielectric layer with the specified thickness to work properly. The second is the utilization of the proper thick EO crystal substrates attached to the thin EO crystal in order to postpone the multiple time delayed reflections in time. However, this requires a properly adhesion between the particular selected thick EO crystal substrate and the thin EO crystal, and it is also not good for time-resolved measurements with sub-picosecond pulses. The third is to eliminate the multiple reflections by improving the refractive index matching at the interface of the thin EO crystal and air via a properly chosen thin conductive layer, which could be selected from a wide range of conductive materials with moderate conductivity and long-term stability, although this layer will absorb part of the incident THz energy. Very recently, the self-referenced method[39] came out and provided a mechanism to remove the effects of echoes, which enables arbitrary temporal window length and, thus, achieves high-resolution frequency.

All in all, as an advanced analytical technological method applicable to a wide variety of materials, THz-TDS has presented unprecedented sensing capabilities for many research fields involving monitoring, sensing, and testing. Nevertheless, it is obvious that higher-power and compact THz sources, more sensitive and broadband THz detectors with good SNR are highly desirable and the primary goals for further development of THz technology.

6. Conclusion

In this paper, the major techniques to generate and detect THz radiation have been reviewed firstly. And

then, in particularly, a number of issues relevant to generation and detection of broadband pulsed THz radiation based on ultra-short pulsed laser as well as broadband time-domain THz spectroscopy (THz–TDS) have been discussed. Concretely, the time-domain waveforms of coherent ultra-short THz pulses from photoconductive antenna excited by femtosecond laser with different pulse durations and their Fourier-transformed spectra have been calculated via the numerical simulation of ultrafast dynamics between femtosecond laser pulse and photoconductive material. The origins of fringes modulated on the top of broadband amplitude spectrum detected by electric-optic sampling using thin nonlinear crystal have been analyzed and the major solutions to get rid of these fringes are discussed.

This work was supported by the National Basic Research Program of China (No. 2007CB310405), the "Hundreds of Talents Programs" of the Chinese Academy of Sciences (No. J08-029), the Innovative Project of the Chinese Academy of Sciences (No. YYYJ-1123), and the CAS/SAFEA International Partnership Program for Creative Research Teams.

References

1. E. Berry and J. Biol, Phys. **29,** 263 (2003).
2. A. G. Davies, A. D. Burnett, W. H. Fan, E. H. Linfield, and J. E. Cunningham, Materials Today **11,** 18 (2008).
3. P. Coward and R. Appleby, in *Proceedings of SPIE: Passive Millimeter-Wave Imaging Technology VI and Radar Sensor Technology VII* **5077,** 54 (2003).
4. C. Zandonella, Nature **424,** 721 (2003).
5. J. Liu, W. Fan, and B. Xue, Chin. Opt. Lett. **9,** S10202 (2011).
6. S. Hadjiloucas, L. S. Karatzas, and J. W. Bowen, IEEE Trans. Microwave Theory Tech. **47,** 142 (1999).
7. P. Y. Han, G. C. Cho, and X.-C. Zhang, Opt. Lett. **25,** 242 (2000).
8. M. Walther, B. M. Fischer, and P. U. Jepsen, Chem. Phys. **288,** 261 (2003).
9. L. B. Braly, K. Liu, M. G. Brown, F. N. Keutsch, R. S. Fellers, and R. J. Saykally, J. Chem. Phys. **112,** 10314 (2000).
10. B. M. Fischer, M. Walther, and P. U. Jepsen, Phys. Med. Biol. **47,** 3807 (2002).
11. Z. Zheng, W. Fan, and B. Xue, Chin. Opt. Lett. **9,** S10506 (2011).
12. H. Harde, R. A. Cheville, and D. Grischkowsky, J. Phys. Chem. A **101,** 3646 (1997).
13. D. M. Mittleman, R. H. Jacobsen, R. Neelamani, R. G. Baraniuk, and M. C. Nuss, Appl. Phys. B **67,** 379 (1998).
14. H. Harde, J. Zhao, M. Wolff, R. A. Cheville, and D. Grischkowsky, J. Phys. Chem. A. **105,** 6038 (2001).
15. R. H. Jacobsen, D. M. Mittleman, and M. C. Nuss, Opt. Lett. **21,** 2011 (1996).
16. B. M. Fischer, M. Hoffmann, H. Helm, G. Modjesch, and P. U. Jepsen, Semicond. Sci. Technol. **20,** S246 (2005).
17. M. van Exter and D. Grischkowsky, Appl. Phys. Lett. **56,** 1694 (1990).
18. T.-I. Jeon and D. Grischkowsky, Phys. Rev. Lett. **78,** 1106 (1997).
19. J. Ng and D. Abbott, Microelectron. J. **33,** 171 (2002).
20. B. E. Cole, J. B. Williams, B. T. King, M. S. Sherwin, and C. R. Stanley, Nature **410,** 60 (2001).
21. H. S. Brandi, A. Latgé, and L. E. Oliveira, Phys. Rev. B **68,** 233206 (2003).
22. E. J. Singley, M. Abo-Bakr, D. N. Basov, J. Feikes, P. Guptasarma, K. Holldack, H. W. Hübers, P. Kuske, Michael C. Martin, W. B. Peatman, U. Schade, and G. Wüstefeld, Phys. Rev. B **69,** 092512 (2004).
23. A. B. Hummel, T. Bauer, E. Mohler, and H. G. Roskos, J. Phys.: Condens. Matter **18,** 2487 (2006).
24. T. Bartel, P. Gaal, K. Reimann, M. Woerner, and T. Elsaesser, Opt. Lett. **30,** 2805 (2005).
25. X. Xie, J. Dai, and X. Zhang, Phys. Rev. Lett. **96,** 075005 (2006).
26. J. Dai, N. Karpowicz, and X. Zhang, Phys. Rev. Lett. **103,** 023001 (2009).
27. R. Köhler, A. Tredicucci, F. Beltram, H. E. Beere, E. H. Linfield, A. G. Davies, D. A. Ritchie, R. C. Iotti, and F. Rossi, Nature **417,** 156 (2002).
28. M. A. Belkin, F. Capasso, A. Belyanin, D. L. Sivco, A. Y. Cho, D. C. Oakley, C. J. Vineis, and G. W. Turner, Nature Photonics **1,** 288 (2007).
29. N. Yu, Q. Wang, M. A. Kats, J. A. Fan, S. P. Khanna, L. Li, A. G. Davies, E. H. Linfield, and F. Capasso, Nature Materials **9,** 730 (2010).
30. H. Chen, W. J. Padilla, J. M. O. Zide, A. C. Gossard, A. J. Taylor, and R. D. Averitt, Nature **444,** 597 (2006).
31. H. Chen, W. J. Padilla, M. J. Cich, A. K. Azad, R. D. Averitt, and A. J. Taylor, Nature Photonics **3,** 148 (2009).
32. F. Miyamaru, M. W. Takeda, and K. Taima, Appl. Phys. Express **2,** 042001 (2009).
33. P. C. Upadhya, W. Fan, A. Bumett, J. Cunningham, A. G. Davies, E. H. Linfield, J. Lloyd-Hughes, E. Castro-Camus, M. B. Johnston, and H. Beere, Opt. Lett. **32,** 2297 (2007).
34. J. Hebling, K. Yeh, M. C. Hoffmann, B. Bartal, and K. A. Nelson, J. Opt. Soc. Am. B **25,** B6 (2008).
35. J. Liu, J. Dai, S. L. Chin, and X. Zhang, Nature Photonics **4,** 627 (2010).
36. H. Schneider, H. Liu, S. Winnerl, C. Song, M. Walther, and M. Helm, Opt. Express **17,** 12279 (2009).
37. S. Komiyama, O. Astafiev, V. Antonov, T. Kutsuwa, and H. Hirai, Nature **403,** 405 (2000).
38. W. H. Fan, A. D. Burnett, P. C. Upadhya, J. E. Cunningham, E. H. Linfield, and A. G. Davies, Applied Spectroscopy **61,** 638 (2007).
39. A. Redo-Sanchez and X. Zhang, Opt. Lett. **36,** 3308 (2011).